Spin waves in one-dimensional bicomponent magnonic quasicrystals

J. Rychły,* J. W. Kłos,† M. Mruczkiewicz, and M. Krawczyk‡
Faculty of Physics, Adam Mickiewicz University in Poznan, Umultowska 85, Poznań, 61-614, Poland
(Received 22 December 2014; revised manuscript received 15 July 2015; published 10 August 2015)

We studied a finite Fibonacci sequence of Co and Py stripes aligned side by side and in direct contact with each other. Calculations based on a continuous model, including exchange and dipole interactions, were performed for structures feasible for fabrication and characterization of the main properties of magnonic quasicrystals. We have shown the fractal structure of the magnonic spectrum with a number of magnonic gaps of different widths. Moreover, localization of spin waves in quasicrystals and the existence of surface spin waves in finite quaiscrystal structure is demonstrated.

DOI: 10.1103/PhysRevB.92.054414 PACS number(s): 75.30.Ds, 75.50.Kj, 75.75.−c, 75.78.−n

I. INTRODUCTION

Quasicrystals [1,2] are aperiodic structures with long range order which can be constructed in deterministic way by self-similar replication or by partial projection of appropriate periodic structure from higher dimensions [3]. This symmetry can be revealed in diffraction pattern showing the set of discrete diffraction spots. The diffraction pattern can be described by the structure factor which, for a quasiperiodic lattice, consists of a dense set of delta peaks. The location and the amplitude of peaks of the structure factor is, on the other hand, related to the position and width of frequency/energy gaps [2]. This feature of quasicrystals allows for advanced tailoring of the band structure which exceeds possibilities offered by homogeneous material or artificial crystals [4,5].

One-dimensional (1D) quasicrystals in the form of the Fibonacci sequence have already been studied for photonic [3,6], electronic [7,8], and phononic [9] systems. However, research of spin waves (SWs) in 1D magnonic quasicrystals (MQs) has been so far mainly limited to theoretical investigations of multilayered structures [10]. Attention was focused on lattice models for exchange SWs [11,12] and in a continuous model for magnetostatic SWs [13]. Recently, SW excitations in quasicrystals were investigated experimentally regarding their localization properties in two-dimensional structures made of thin veins of Py [14,15] and in a larger scale for enhancement of nonlinear effects in thick yttrium-iron-garnet film with a Fibonacci sequence of etched groves [16]. These studies have shown interesting properties of MQs potentially useful for applications and fundamental studies. However, there is an evident gap in studies of SW dynamics in MQs, especially in studies of structures feasible for experimental realization. This area can be explored theoretically by considering the finite structure of planar geometry and including both exchange and dipole interactions. Therefore, we focus our study on planar bicomponent MQs modulated in nanoscale, i.e., on structures preserving all features characteristic for wave dynamics in quasiperiodic structures which are possible for fabrication and characterization.

We considered a thin plate of 1D MQs in the form of a finite Fibonacci sequence consisting of Co and permalloy (Py: $Ni_{80}Fe_{20}$) stripes. Ferromagnetic stripes were in direct contact, which ensures exchange coupling between neighboring stripes, in addition to long-range dipole interactions. We investigated a system in a saturation state with static magnetization aligned along infinite stripes. The strong dynamical coupling makes the system dispersive for propagating SWs with interesting features like a fractal SW spectra and localized properties of SWs. Moreover, the finite Fibonacci sequence allowed us to study surface SWs localized at the edges of the MQs. To find frequencies of SWs and their spatial profiles we solved a linearized Landau-Lifshitz equation with the finite-element method (FEM) in the frequency domain [17,18].

First, we present the structures under investigation and describe shortly the computational method we used (Sec. II). In Sec. III we present results of our calculations and perform discussion of obtained results. Finally, in the last section, we summarize the paper.

II. MODEL AND THE STRUCTURE

We have investigated SW spectra for 1D MQs obtained according to the Fibonacci inflation rule and made from long Co and Py stripes of 91 nm width and 30 nm thickness. The saturation magnetization and exchange constants for Co and Py are as follows: $M_{\mathrm{Py}} = 0.86 \times 10^6$ A/m, $A_{\mathrm{Py}} = 1.3 \times 10^{-11}$ J/m, $M_{\mathrm{Co}} = 1.445 \times 10^6$ A/m, and $A_{\mathrm{Co}} = 3.0 \times 10^{-11}$ J/m [19,20]. For each material gyromagnetic ratio $\gamma = 176$ GHz/T is assumed the same. In accordance with the Fibonacci inflation rule, Co and Py stripes are arranged in Fibonacci sequence using the following recursion: $S_n = [S_{n-1}S_{n-2}]$ [21], where S_1 and S_2 are initial structures consisting of single-Co and -Py stripes, respectively. $[S_{n-1}S_{n-2}]$ indicates concatenation of the two subsequences S_{n-1} and S_{n-2} of the stripes. We obtained in the first subsequences: Co, Py, PyCo, PyCoPy, and PyCoPyPyCo [Fig. 1(a)]. In each next step the structure total width grows in the x direction, e.g., for the quasicrystal made from 55 stripes the width of the whole structure is 5 μm. We have analyzed structures S_{10}, S_{11}, ..., S_{16}, made of 55, 89, 144, 233, 377, 610, and 987 numbers of stripes, respectively. With $n \to \infty$ the filling fraction of the Py approach to the golden ratio $\sigma = (\sqrt{5}-1)/2$ and the sequence of stripes S_∞ becomes rigorously quasiperiodic. We use the coordinate system as defined in Fig. 1. Along stripes structure is infinite

*rychly@amu.edu.pl
†klos@amu.edu.pl
‡krawczyk@amu.edu.pl

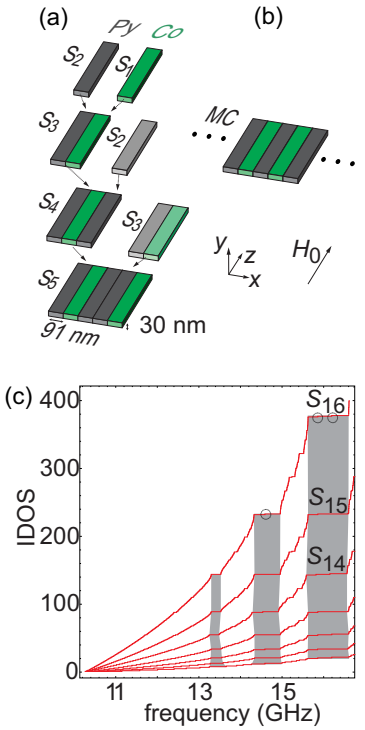

FIG. 1. (Color online) (a) First few sequences of a planar Fibonacci MQ (Fibonacci sequences from S_1 to S_5 are shown) composed of Py and Co infinite stripes of finite width and thickness. (b) 1D bicomponent magnonic crystal (MC) with Py and Co infinite stripes of the same width. Both structures are saturated by external magnetic field H_0. (c) Integrated density of states (IDOS) as a function of frequency for successive Fibonacci sequences: from S_{10} (bottom curve) to S_{16} (top curve). In the IDOS of the S_{16} MQ three surface SWs existing in the widest magnonic gaps are marked with circles.

and saturated by the external magnetic field $\mu_0 H_0 = 0.1$ T. To emphasize interesting properties of SWs in quasicrystals we will make reference to magnonic spectra calculated for magnonic crystal (MC) [22] composed of the same stripes of Py and Co as in the Fibonacci sequence [Fig. 1(b)].

To calculate SW spectra we solve the Landau-Lifshitz equation (LLE):

$$\frac{\partial \mathbf{M}(\mathbf{r},t)}{\partial t} = \mu_0\gamma[\mathbf{M}(\mathbf{r},t) \times \mathbf{H}_{\text{eff}}(\mathbf{r},t) + \frac{\alpha}{M_S}\mathbf{M}(\mathbf{r},t) \times (\mathbf{M}(\mathbf{r},t) \times \mathbf{H}_{\text{eff}}(\mathbf{r},t))], \quad (1)$$

where t is time and $\mathbf{r}$ is position vector. The last term describes damping of SWs with α being the dimensionless damping coefficient. $\mathbf{H}_{\text{eff}}$ is an effective magnetic field, which is assumed to be the sum of three terms: $\mathbf{H}_{\text{eff}} = \mathbf{H}_0 + \mathbf{H}_{\text{ex}} + \mathbf{H}_{\text{dm}}$. $\mathbf{H}_{\text{ex}}$ is an exchange field and $\mathbf{H}_{\text{dm}}$ is a dynamic demagnetizing field with components along the x and y directions (due to assumed geometry the static demagnetizing field is 0). The $\mathbf{H}_{\text{ex}}$ and $\mathbf{H}_{\text{dm}}$ fields are defined in Ref. [17]. We neglect the magnetic anisotropy term in $\mathbf{H}_{\text{eff}}$, because its influence on the presented results in MQs and MCs composed of Py and Co nanostripes is small [23].

From Eq. (1) we find dynamical components of magnetization, $\mathbf{m}(\mathbf{r},t)$ [$\mathbf{M}(\mathbf{r},t) = M_z(\mathbf{r})\mathbf{e}_z + \mathbf{m}(\mathbf{r},t)$]. We use a linear approximation, i.e., we neglect the higher-order terms arising in Eq. (1) with respect to $\mathbf{m}$. This is justified when M_z is assumed to be constant in time, namely when $|\mathbf{m}(\mathbf{r},t)| \ll M_z\mathbf{e}_z$, and therefore $M_z \approx M_S$ (M_S is saturation magnetization). We seek solutions of LLE (1) in the form of monochromatic SWs, having harmonic dynamics in time: $e^{i\omega t}$, where ω is angular frequency of the SW. Equation (1) is complemented with Maxwell equations to determine demagnetizing fields. With these equations, we define the eigenvalue problem, which is solved by using FEM with COMSOL 4.3a software to obtain dispersion relation and profiles of SWs. For more details concerning this computation we refer to Ref. [18]. From the solution of Eq. (1) we found complex values of ω with its real part corresponding to SW frequency and its imaginary part proportional to the inverse of time of life of the SW [24]. We have checked numerically that the influence of damping on SW frequencies (by assuming α coefficients 0.01 and 0.1 for Py and Co, respectively, in one calculations and 0 in other) is smaller than 0.5% [25]. Thus, in further calculations we neglect damping.

III. RESULTS AND DISCUSSION

To visualize the SW spectra we use the integrated density of states (IDOS), defined as:

$$\text{IDOS}(f_i) = \sum_{j=0}^{i} \text{DOS}(f_j), \quad (2)$$

where DOS is density of SW modes and f_i is a frequency of the ith SW mode ($f_i = \omega_i/2\pi$), which are ordered according with increased frequency [26]. IDOS as a function of frequency calculated for successive Fibonacci sequences from S_{10} to S_{16} are shown in Fig. 1(c).

Due to the finite width of structures used in calculations, we always observe a discrete set of frequencies. The finer steps and faster increase of IDOS are observed for wider structures (i.e. composed of larger number of nanostripes). By finding plateaus in IDOS we are able to identify magonic gaps. The width of these plateaus converges for larger Fibonacci structures and can approximate width of magnonic gaps in infinite MQs [see the gray areas marked in Fig. 1(c)]. Within some plateaus of IDOS, we can also find surface modes of MQs. In IDOS shown in Fig. 1(c) these surface SWs are indicated by separated steps (marked with circles for S_{16}) inside the magnonic gaps, discussed in a later part of the paper.

With the increase (decrease) of size of the structure, the spectrum of IDOS reveals more (less) details which are characteristic for quasicrystals [see Fig. 1(c)]. For larger structures, we are able to identify the fine structure of magnonic gaps, whereas gaps found for shorter sequences still exist [27]. This provides us with a mechanism to explore the fractal nature of the SW spectrum in MQs. In Fig. 2(a) we present in detail the spectrum for structure consisting of 377 nanostripes. The inset in this figure shows a magnified region of spectrum with a subtle, multilevel structure of magnonic gaps, resembling the property of self-similarity.

In order to validate the fractal nature of the SW spectrum we have calculated its Hausdorff dimension [28]. We divided the whole investigated frequency range into intervals of equal lengths Δf and then we counted the number $N(\Delta f)$ of

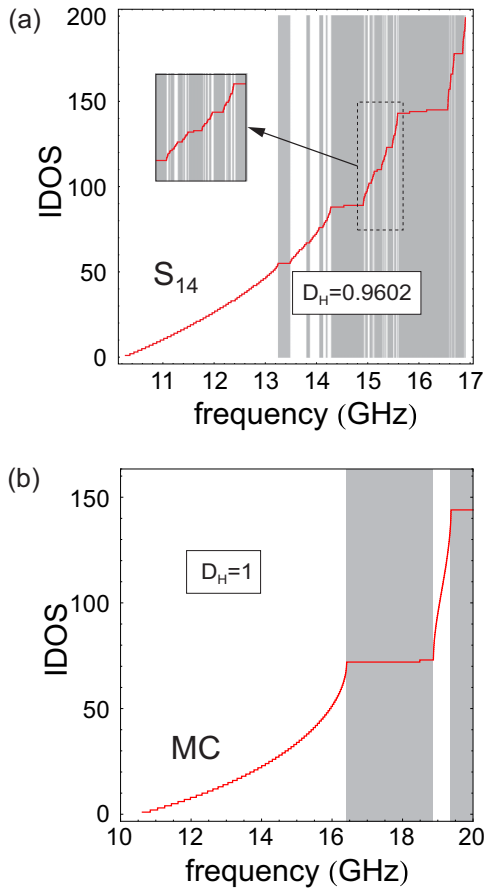

FIG. 2. (Color online) (a) IDOS for Fibonacci sequence S_{14}. Gray areas mark the most pronounced magnonic gaps. Inset presents the magnified region of the IDOS plot where the complex band-gap structure is visible. The Hausdorff dimension D_H is equal to 0.9602. (b) IDOS for MC consisting of 144 nanostripes, $D_H = 1$.

these intervals which are included in or partially overlap with magnonic bands. The number $N(\Delta f)$ increases with a decrease of length Δf and the dependence of $\log[N(\Delta f)]$ on $\log(\frac{f_0}{\Delta f})$ should be linear (f_0 is a frequency of the first mode in spectra, and its choice is arbitrary and does not influence results). The Hausdorff dimension of the spectrum is defined as the derivative:

$$D_H = \frac{d\ \log[N(\Delta f)]}{d\ \log\left(\frac{f_0}{\Delta f}\right)}. \tag{3}$$

Numerically, we have calculated D_H as a coefficient of regression for dependence of $\log[N(\Delta f)]$ on $\log(\frac{f_0}{\Delta f})$. We have obtained the value $D_H = 0.9603$ with the standard deviation 0.0011 and the coefficient of regression $R^2 = 0.99991$, which points close to linear dependence. This noninteger value of D_H proves the fractal property of the SW spectra in MQs. Its value is close to the D_H obtained for plasmonic Fibonacci structures [28]. In the considered range of frequencies (which is accessible for experimental investigations) we found the D_H practically independent on the size of intervals Δf. This indicates that the spectrum is not a multifractal one and can be characterized by a single D_H dimension.

The IDOS for MCs has a regular dependence on f. In Fig. 2(b) we have plotted the IDOS(f) for a MC structure consisting of 144 nanostripes. Here D_H is equal to 1. The first magnonic band gap starts at 16.5 GHz; however, in MQ gaps are present already at the lower frequencies. The existence of low-frequency gaps in MQs can be useful for application, for instance, in magnon transistors [29].

The other interesting issue of excitations in quasicrystals is a possibility for their spatial localization in MQ interiors [6]. In crystals without any defects, all modes are extended, but in random systems localization occurs [30,31]. MQs are neither periodic nor random systems. Therefore, we can observe both extended and localized SW modes.

To discuss localization quantitatively, we need a measure of the strength of localization. For this purpose we will use localization factor λ [32]. The parameter λ_i for the ith mode is defined as:

$$\lambda_i = \frac{1}{L}\sum_{j=0}^{j=L} \log|m_{x,i}(x_j)|, \tag{4}$$

where the in-plane dynamical component of magnetization $m_{x,i}(x_j)$ is taken at the point x_j and is normalized according with the norm:

$$\frac{1}{L}\sum_{j=0}^{j=L} |m_{x,i}(x_j)| = 1. \tag{5}$$

Summation runs over all L equidistant points x_j covering all the space between surfaces of the structure along x axis. The $\lambda = 0$ corresponds to uniform excitation. For all other modes λ takes negative values. Modes with stronger localization are characterized by a large absolute value of λ.

In the considered systems, the separation of frequencies of SW modes quantized across the thickness, exceeds the frequency range considered in this paper. Thus, for further analysis of localization factors, we take SW amplitude from the middle plane of the structure.

Localization factors of SWs in MC and the Fibonacci quasicrystal (S_{12}) are shown in Fig. 3. In general, the localization factor λ increases in magnitude with growing frequency. For extended modes (e.g., in MCs or the low-frequency part of the MQ spectra) with increasing frequency, the number of nodal points in the profiles of the SWs increases (see the profiles of the SWs in Fig. 3). Because Py has lower ferromagnetic resonance frequency than Co, the modes distribute their amplitude more in Py stripes with nodal points placed mainly in Co stripes. Such inhomogeneous distribution increases the magnitude of λ. The rate of this change is relatively small for MC [see Fig. 3(b)] where the localization factor for SWs up to 20 GHz does not fall below -1 (apart from mode 73 being a surface SW, which is discussed later). In the case of MQs [S_{12} shown in Fig. 3(a)], changes of the measure of localization have a tendency similar to that for MC to $\approx$15 GHz.

Modes corresponding to higher frequencies feel the structure stronger and, because of that, they oscillate more sharply than modes corresponding to lower frequencies. The Fibonacci sequence is much more complex than a periodic one, thus the high-frequency excitations essentially differ more for MQs than for MCs. There are three reasons for this: (i) in MQs Py stripes of both single (91 nm) and double (182 nm) widths are present [see Fig. 1(a)], (ii) the Py and Co stripes are distributed

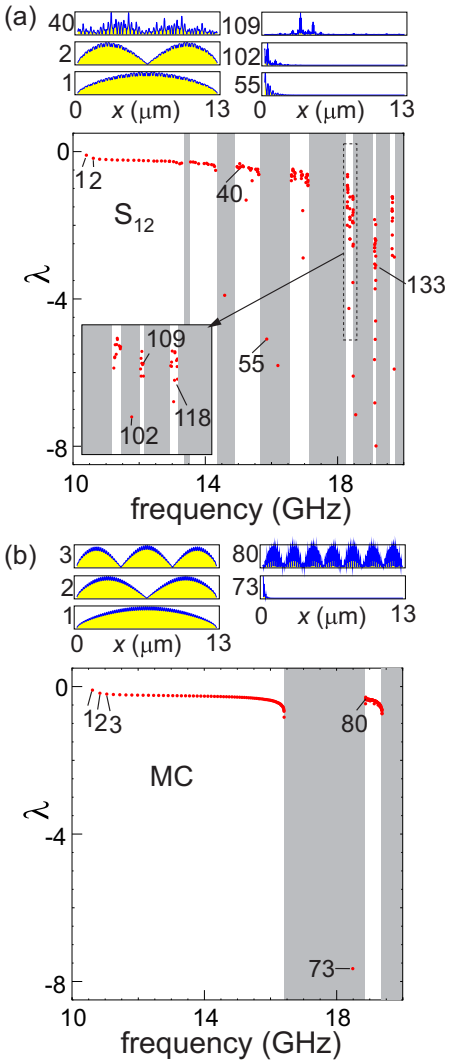

FIG. 3. (Color online) Localization factors λ of SW modes in (a) the S_{12} sequence of the Fibonacci MQs and (b) of MC composed of the same number of nanostripes in dependence on frequency. Numbers labeling points in the (λ, f) plot denote successive numbers of modes ordered with increased frequency. Profiles of the modulus of the x component of magnetization along the structure are plotted in insets above the main plot. The region of the selected band in (a) is magnified in the separate inset. Gray areas denote magnonic gaps of the widest width.

quasiperiodically within the MQ, and (iii) the neighborhood of each stripe can differ for MQs, while it is always the same for MC. In the considered, higher-frequency range, modes are concentrated in selected single- or double-Py stripes in MQs. The first group of modes above the extended mode range consists of modes with the amplitude concentrated in some double-width Py stripes with one nodal point in each Py stripe. Then there is a group of modes with two nodal points in the double-Py stripe, i.e., a second harmonic of the double stripe (e.g., modes 109 and 118 in Fig. 4) and then group of modes concentrated in a few single-Py stripes with one nodal point within the Py stripe, e.g., mode 133.

Each of the above-discussed localized bulk modes is located at given sets of positions (single- or double-Py stripes), mostly

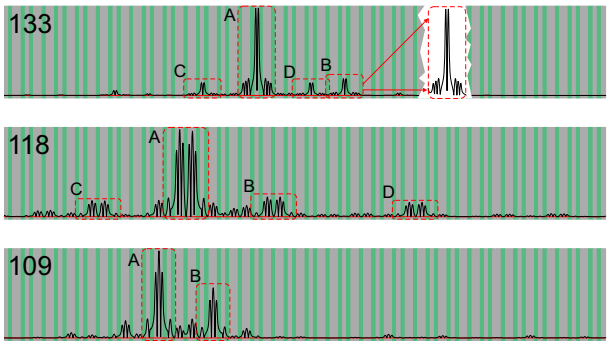

FIG. 4. (Color online) The profiles of the modulus of the x component of magnetization in S_{12} Fibonacci MQs for the bulk modes 109, 118, and 133, labeled in Fig. 3(a). The gray and green bars in the background mark the regions of Py and Co, respectively. The letters A, B, C, and D denote the areas (marked with dashed lines) of SW localization with similar surroundings. For mode 133 the amplitude from the B area is zoomed in and shown on the white background.

because of the similarities between surroundings of positions of SW amplitude localizations. For a selected frequency, at most a few Py stripes with very similar surroundings are able to hold the same excitation. In Fig. 4 we analyze in detail the selected profiles of those bulk modes (modes 109, 118, and 133), localized within the S_{12} MQ, as they are the modes of higher frequencies (18.37, 18.47, and 19.13 GHz, respectively). The highest amplitude for mode 109 is observed in the double-width Py stripes. We mark the two locations A and B with the highest amplitude of the SWs. By zooming in less intense excitation at location B we noticed that it has the same spatial profile as the most intense excitation from location A. This similarity can be explained by inspecting the neighborhood of these two locations. For location A the following sequence of single- (s) and double- (d) width Py stripes can be found: $|\boldsymbol{s}dsddsdsddsdds\mathrm{A}s\boldsymbol{d}dsddsdsddsdsdsddsd\boldsymbol{d}$. The symbol | denotes the surface of the structure. By swapping the left and right surroundings of B the following sequence of stripes could be found: $ds\boldsymbol{d}dsddsdsddsdds\mathrm{B}s\boldsymbol{d}dsddsdsddsdsdsddsd\boldsymbol{s}$. It is easy then to notice that the sequences of stripes in the neighborhoods of locations A and B differ at very far positions (i.e., at positions 14 and 19 from the positions of A and B), which are marked with bold letters in the sequences. A similar discussion can be conducted for modes 118 and 133. It also could be noted that mode 118 is concentrated in the two double-Py stripes separated by the single Co stripe, whereas mode 133 is concentrated within one single Py stripe.

It was shown that for photonic and electronic structures the localization of the modes in the Fibonacci structures is supposed to be weaker than exponential and is governed by a power-law dependence [33,34]. This property makes them substantially different from either defect modes in disordered structures resulting from Anderson localization or surface modes in periodic systems induced by termination of the structure. We expect that these "chaotic" modes [21] will have self-similar properties [34] also for magnonic systems.

We discuss now the modes with amplitude localized at the surface of the structure, i.e., the surface states, found in MC and MQ spectra. Occurrence of surface modes is determined

mostly by the element placed on the surface of the crystal (in our case it is the single stripe of Py) and its frequency overlapping with the gap [35]. Only up to two surface modes structured on the basis of the excitation with fixed quantization in the surface stripe (i.e., with fixed number of nodes in the Py stripe) can occur. The SW spectrum of the finite Fibonacci structure contains many surface modes which exist in frequency gaps, appearing in large numbers in comparison to the periodic structure. Additionally, it is important to notice that the amplitude of surface waves penetrate to the inside of the structure, which also has an impact on the properties of excitation. Because of that, surface modes appearing in MCs and MQs could differ, regardless of the same surface element and amplitude distribution in this element. In MC we have found only one surface mode up to 20 GHz [mode 73 in Fig. 3(b)] but in MQs, many surface modes can be identified [e.g., mode 55 shown in Fig. 3(a)]. They have $\lambda < -4$, which exceeds the factor of bulk modes. For some modes with a frequency near the end of the bunch of bulk modes (e.g., mode 102) distinguishing between the bulk and surface characters can be ambiguous. We can point out that the strength of the localization of the surface modes increases if its frequency is located in the center of the gap, when this gap is wider, and when its frequency is high.

Finally, we discuss the long-wavelength part of the spectra. In the low-frequency limit, both periodic and Fibonacci structures exhibit similar properties: much of the same profiles [see the insets in Figs. 3(a) and 3(b) for modes 1 and 2], frequencies, and localization factors of the SWs [compare Figs. 3(a) and 3(b)]. In this limit both systems can be treated as metamaterials characterized by effective magnetic properties [36]. It is worth noting that, in this limit, the IDOS(f) spectra of MQs and MCs have features characteristic for the Damon-Eshbach wave in homogeneous film [19,20].

We have proposed the MQ composed of Py and Co stripes suitable for experimental study of fractal properties in magnonics. Indeed, the magnonic band structure has already been investigated in MCs composed of Py or Co and Py stripes with periodicity $\propto$500 nm and interesting physical properties, like magnonic band gaps and reprogrammability, have been demonstrated [19,37–39]. Brillouin light scattering (BLS) to measure dispersion relations of SWs, micro-BLS spectroscopy [40], and time-resolved magneto-optical Kerr effect (TR-MOKE) microscopy [41,42] with spatial resolution down to 250 nm, to visualize profiles of SW excitations, have been used. These techniques can be directly implemented to study SWs in MQs to confirm predicted properties. The area of SW localization in the MQs under investigation spreads over a few Py stripes [e.g., modes 55, 102, and 109 in Fig. 3(a)], which is above the limits of the spatial resolution in the BLS and TR-MOKE microscopes. Such direct studies of SW localization are extremely difficult for layered systems but can be performed for considered structures of in-plane periodicity. Moreover, properties of SWs in MQs presented above preserve also in larger structures, i.e., with stripe width extended up to few hundred nm. To confirm this we present, in Fig. 5, IDOS as a function of frequency calculated for MQs composed of 250 nm width Py and Co stripes, i.e., the size that exactly matches the stripes of the MCs studied in Ref. [19]. The obtained spectrum is shifted to frequencies lower than in the case of MQs with stripes of 91 nm width [Fig. 2(a)]. It has the same fractal structure, which is confirmed by a slightly smaller Hausdorff dimension, $D_H = 0.9413$.

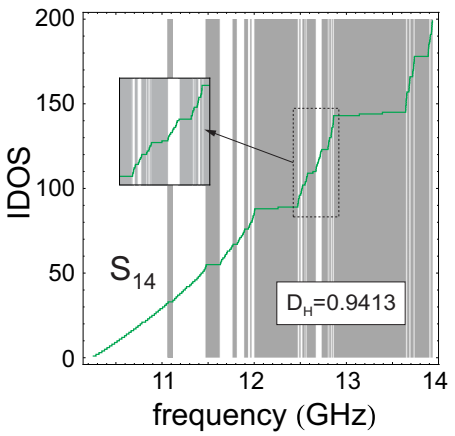

FIG. 5. (Color online) IDOS of the Fibonacci sequence S_{14} composed of wide Py and Co stripes of 250 nm width and 30 nm thickness. Gray areas mark the most pronounced magnonic gaps. The inset presents the magnified region of IDOS plot where the complex band-gap structure is visible. The Hausdorff dimension of the spectrum is equal to $D_H = 0.9413$.

IV. SUMMARY

We have theoretically investigated periodic and quasiperiodic planar magnonic systems suitable for experimental realization. Fibonacci and periodic structures which consist of thin Py and Co stripes where considered. We have shown that the spectrum of IDOS for MQ systems exhibits a complex, multilevel structure of frequency gaps with finer details revealed for long Fibonacci sequences. Calculated magnonic spectra form a fractal set with a self-similarity property characterized by the Hausdorff dimension $D_H = 0.9602$. Computed localization factors allow us to discuss quantitatively the strength of localization of SWs in MQs. We have shown the localization of the bulk modes in quasiperiodic systems and its enhancement for higher frequencies, where the spectrum of Fibonacci structures becomes substantially complex. The presence of multiple magnonic gaps supports also the existence of surface SWs that are observed numerously in MQs. In the long-wavelength limit both MQs and MCs preserve similar effective properties. Obtained results show that quasicrystal structures can be investigated in magnonics with standard experimental techniques and their fractal properties can be explored.

ACKNOWLEDGMENTS

The authors thank Dr Andriy E. Serebryannikov for fruitful discussions. The presented research received funding from Polish National Science Centre Project No. DEC-2-12/07/E/ST3/00538, project SYMPHONY (program TEAM/2011-8/4) of the Foundation for Polish Science, and from the EUs Horizon2020 research and innovation program under Marie Skłodowska-Curie GA No. 644348.

[1] D. Levine and P. J. Steinhardt, Phys. Rev. Lett. **53**, 2477 (1984).

[2] C. Janot, *Quasicrystals: A Primer*, 2nd ed. (Oxford University Press, Oxford, 1994).

[3] Z. V. Vardeny, A. Nahata, and A. Agrawal, Nat. Photon. **7**, 177 (2013).

[4] E. Macia, Rep. Prog. Phys. **69**, 397 (2006).

[5] T. Janssen and A. Janner, Acta Cryst. B **70**, 617 (2014).

[6] M. Kohmoto, B. Sutherland, and K. Iguchi, Phys. Rev. Lett. **58**, 2436 (1987).

[7] R. Merlin, K. Bajema, Roy Clarke, F.-Y. Juang, and P. K. Bhattacharya, Phys. Rev. Lett. **55**, 1768 (1985).

[8] F. Laruelle and B. Etienne, Phys. Rev. B **37**, 4816(R) (1988).

[9] W. Steurer and D. Sutter-Widmer, J. Phys. D: Appl. Phys. **40**, R229 (2007).

[10] E. L. Albuquerque and M. G. Cottam, Phys. Rep. **376**, 225 (2003).

[11] C. H. O. Costa and M. S. Vasconcelos, J. Phys.: Condens. Matter **25**, 286002 (2013).

[12] T. S. Liu and G. Z. Wei, Phys. Rev. B **48**, 7154 (1993).

[13] D. H. A. L. Anselmo, M. G. Cottam, and E. L. Albuquerque, J. Appl. Phys. **85**, 5774 (1999).

[14] V. S. Bhat, J. Sklenar, B. Farmer, J. Woods, J. T. Hastings, S. J. Lee, J. B. Ketterson, and L. E. De Long, Phys. Rev. Lett. **111**, 077201 (2013).

[15] V. S. Bhat, J. Sklenar, B. Farmer, J. Woods, J. B. Ketterson, J. T. Hastings, and L. E. De Long, J. Appl. Phys. **115**, 17C502 (2014).

[16] S. V. Grishin, E. N. Beginin, Yu. P. Sharaevskii, and S. A. Nikitov, Appl. Phys. Lett. **103**, 022408 (2013).

[17] M. Mruczkiewicz, M. Krawczyk, V. K. Sakharov, Yu. V. Khivintsev, Yu. A. Filimonov, and S. A. Nikitov, J. Appl. Phys. **113**, 093908 (2013).

[18] M. Mruczkiewicz, M. Krawczyk, G. Gubbiotti, S. Tacchi, Yu. A. Filimonov, D. V. Kalyabin, I. V. Lisenkov, and S. A. Nikitov, New J. Phys. **15**, 113023 (2013).

[19] Z. K. Wang, V. L. Zhang, H. S. Lim, S. C. Ng, M. H. Kuok, S. Jain, and A. O. Adeyeye, Appl. Phys. Lett. **94**, 083112 (2009).

[20] M. L. Sokolovskyy and M. Krawczyk, J. Nanopart. Res. **13**, 6085 (2011).

[21] M. Kohmoto, B. Sutherland, and C. Tang, Phys. Rev. B **35**, 1020 (1987).

[22] M. Krawczyk and D. Grundler, J. Phys.: Condens. Matter **26**, 123202 (2014).

[23] According to experimental studies in MCs composed of polycrystalline Co and Py nanostructures deposited with electron beam lithography, magnetocrystalline, and magnetic anisotropy from the interface with the substrate is small and have negligible effect on SW dynamics [19,39]. Thus, in our calculations devoted to similar structures we have neglected magnetic anisotropies.

[24] A. G. Gurevich and G. A. Melkov, *Magnetization Oscillations and Waves* (CRC Press, Boca Raton, FL, 1996).

[25] The imaginary part of ω is closer to the respective value of homogeneous Py film than of Co film for SWs investigated in this paper, because the main contribution to these excitations comes from Py. As in planar MCs [19], this damping shall not influence significantly experiments proposed at the end of this paper.

[26] IDOS defined according with Eq. (2) is in fact the sum of the number of SW frequencies up to the frequency f_i.

[27] In Fig. 1(c), we marked magnonic gaps (between frequencies of the last and the first bulk mode in the bands below and above the given gap, respectively). The width of these frequency ranges can by slightly overestimated due to quantization of frequencies.

[28] G. I. Zaginaylov, A. Grudiev, K. Schünemann, and P. V. Turbin, Phys. Rev. Lett. **88**, 195005 (2002).

[29] A. Chumak, A. A. Serga, and B. Hillebrands, Nat. Commun. **5**, 4700 (2014).

[30] E. Abrahams, P. W. Anderson, D. C. Licciardello, and T. V. Ramakrishnan, Phys. Rev. Lett. **42**, 673 (1979).

[31] P. E. Wolf and G. Maret, Phys. Rev. Lett. **55**, 2696 (1985).

[32] W.-C. Xie and I. Elishakoff, Chaos Solitons & Fractals **11**, 1559 (2000).

[33] L. DalNegro, C. J. Oton, Z. Gaburro, L. Pavesi, P. Johnson, A. Lagendijk, R. Righini, M. Colocci, and D. S. Wiersma, Phys. Rev. Lett. **90**, 055501 (2003).

[34] R. B. Capaz, B. Koiller, and S. L. A. de Queiroz, Phys. Rev. B **42**, 6402 (1990).

[35] S. G. Davison and M. Steslicka, *Basic Theory of Surface States* (Oxford University Press, Oxford, 1996).

[36] M. Mruczkiewicz, M. Krawczyk, R. V. Mikhaylovskiy, and V. V. Kruglyak, Phys. Rev. B **86**, 024425 (2012).

[37] J. Topp, D. Heitmann, M. P. Kostylev, and D. Grundler, Phys. Rev. Lett. **104**, 207205 (2010).

[38] J. Ding, M. Kostylev, and A. O. Adeyeye, Phys. Rev. Lett. **107**, 047205 (2011).

[39] S. Tacchi, G. Duerr, J. W. Klos, M. Madami, S. Neusser, G. Gubbiotti, G. Carlotti, M. Krawczyk, and D. Grundler, Phys. Rev. Lett. **109**, 137202 (2012).

[40] M. Madami, G. Gubbiotti, S. Tacchi, and G. Carlotti, Solid State Phys. **63**, 79 (2012).

[41] Y. Au, E. Ahmad, O. Dmytriiev, M. Dvornik, T. Davison, and V. V. Kruglyak, Appl. Phys. Lett. **100**, 182404 (2012).

[42] A. Barman and A. Haldar, Solid State Phys. **65**, 1 (2014).